Synthesis, and Crystal Structure of Phosphates with Yavapaiite Type-structur

Rachid Fakhreddine, My Rachid Tigha, Hajar Bellefqih, Az-Iddin Chham, Noureddine Sajai, Ali Ouasri, Abderrahim Aatiq

Synthesis, and crystal structure of phosphates with yavapaiite type-structure.

Rachid Fakhreddine[1]*(0000-0002-4741-9509), My Rachid Tigha[2], Az-iddin Chham[3], Noureddine Sajai[1], Hajar Bellefqih[2], Ali. Ouasri [4], Abderrahim. Aatiq[2].

[1]Laboratory of Materials Engineering for Environment and Valorization (GeMEV), Faculty of Sciences Aïn Chock, Hassan II University, Casablanca, Morocco.

[2]Laboratory of Physical-Chemistry, Materials and Catalyse (LCPMC), Faculty of Sciences Ben M'Sik, Hassan II University, Casablanca, Morocco.

[3]Laboratory of Organic Synthesis, Extraction and Valorization (SOEV), Faculty of Sciences Aïn Chock, Hassan II University, Casablanca, Morocco.

[4]Laboratory, Centre Regional des Métiers de l'Education et de la Formation (ReSIP), Madinat Al Irfane, Souissi, BP 6210 Rabat, Morocco.

rachidfak@yahoo.fr

Abstract.

The synthesis and structural study of three new $Ba_2SbM(PO_4)_4$ (M= Sc and Yb) phosphates, abbreviated as [Sc] and [Yb], were prepared by solid state reaction in air atmosphere and their structures has been solved ab initio by Rietveld analysis. The three phases crystallize in the Yavapaiite structure with C2/m space group (Z=2), with cell parameters a= 8.292(1) Å; b= 5.234(3) Å c= 7.878(7) Å and β= 93.81(1)° for [Sc], and a= 8.345(1) Å; b= 5.265(3) Å c= 7.977(3) Å and β= 94.22(1) ° for [Yb].

Keywords: Phosphates, solid-state reaction, Rietveld method, Yavapaiite structure.

1   Introduction

The chemistry of double $A^{II}M^{IV}(PO_4)_2$ (A^{II} =Ca, Sr, Pb, Ba; M^{IV} = Ge, Ti, Mo, Sn, Hf, Zr) phosphates have been intensively studied during the past two decades for applications including catalysts, ion conductors, optical [1-6], magnetic [7] and also as potential host matrices for minor actinide immobilization [8–9]. It should be noted that the size of the A^{2+} and M^{4+} cations has a significant effect on the crystal structure. For smaller M^{4+} ions, as in the $BaM^{IV}(PO_4)_2$ (M^{IV}= Ge, Ti, Mo, Sn, Hf, Zr) phases [10-15], the structure is monoclinic and isotypic of the archetype $KFe(SO_4)_2$ yavapaïte phase (*C2/m* space group, Z=2) [16]. For small A^{2+} and M^{4+} cations sizes, as in the case of $SrM^{IV}(PO_4)_2$ (M^{IV} = Ge Phosphates, solid-state reaction, Rietveld method, Yavapaiite structure, Ti, Sn) [11-12] and $PbM^{IV}(PO_4)_2$ (M^{IV} = Ge,Ti) [5], a distorted yavapaiite structure-type

with $C2/c$ space group (Z=4) was reported. Compounds obtained from the coupled substitution of M^{IV} cations, in $A^{II}M^{IV}(PO_4)_2$ compounds, by M'^{III} and M''^{V} ions ($M^{IV}= 0.5M'^{V}+0.5M''^{III}$) as in $Ba(Nb^{V}_{0.50}M''^{III}_{0.50})(PO_4)_2$ (M'^{III} = Al, Cr, Fe, In) and $Ba(Sb^{V}_{0.50}M''^{III}_{0.50})(PO_4)_2$ (M''^{III} = Cr, Ga, Fe) have been synthesized and characterized by some of us [17-21]. The structure of these phases consists of layers of Ba^{2+} cations in tenfold coordination, alternating with dense slabs of $(M'^{V}/M''^{III})O_6$ octahedra and PO_4 tetrahedra interconnected by corner-sharing. In a continuation of our work search, in the present study, we have determined the crystal structure of [Sc] and [Yb] compounds from powder XRD data.

2   Materials and Methods

2.1   Description of the experimental

$Ba_2SbM(PO_4)_4$ (M= Sc, In and Yb) compounds was prepared from stoichiometric amounts of reagent-grade chemicals $BaCO_3$ (Riedel de Haën, 99 %), Sb_2O_3 (Riedel de Haën, 99.9 %), $NH_4H_2PO_4$ (Riedel de Haën, 99 %) and M_2O_3 (M=Sc, Yb) oxides. They were mixed in an agate mortar and putted in an alumina crucible. The mixtures were heated progressively, in a furnace at air atmosphere, with intermittent grinding at 150 °C (24 h), 300 °C (24 h), 400 °C (24 h), 600 °C (24 h), 700 °C (24 h), 800 °C (48 h), and 850°C (48 h).

2.2   X ray powder diffraction

X-ray powder diffraction data for structural determination were collected at room temperature on a Panalytical X'Pert diffractometer in Bragg–Brentano geometry using monochromatized CuKα radiation (45 kV, 40 mA). The data were collected from 10 to 90° (2θ°), in steps of 0.01. Rietveld analyses were carried out with the Fullprof suite program [22].

3   Results and discussion

3.1   Rietveld refinement of $Ba_2SbM(PO_4)_4$ (M= Sc and Yb)

3.1.1 Structural refinement of $Ba_2SbSc(PO_4)_4$

Barium phosphate-type has been reported in several times as fully isotypic with the yavapaiite structure phases [17-20]. Analysis of XRD spectra for the three [Sc] and [Yb] materials indicated that the principal peak positions and their intensity are similar to those observed in the $Ba_2SbFe(PO_4)_4$ XRD phase. Rietveld analysis in Le Bail's (profile matching) mode confirmed that structure of [Sc] phase is compatible with the $C2/m$ space group. So, initial starting parameters for the Rietveld refinement of [Sc] were based on those already reported by Aatiq et al. for $Ba_2SbFe(PO_4)_4$ phase in the $C2/m$ space group (Z = 2) [17]. This refinement leads to acceptable reliability factors (e.g., R_B = 3.2 %). A comparison of the experimental and calculated XRD profile of [Sc] material is given in Fig 1. Obtained crystallographic data and structural parameters are given in Tables 1. Selected interatomic distances and calculated bond valence sum BVS are gathered in Table 2
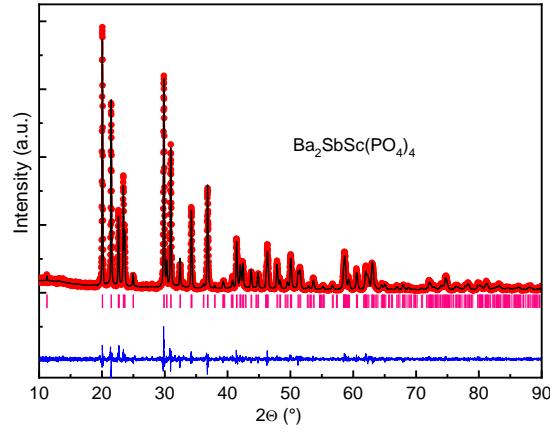
Fig.1. Rietveld refined diffraction patterns of $Ba_2SbSc(PO_4)_4$ phase.

3.1.1 Structural refinement of $Ba_2SbYb(PO_4)_4$

The atomic positions of the $Ba_2SbFe(PO_4)_4$ phase were used as starting structural parameters for the Rietveld refinements of [Yb]. In this case, the pattern indicates the presence of a secondary phase with a small amount (about 8% by weight) which is attributed to $YbPO_4$ (JCPDS PDF#83-0664). Therefore, the Rietveld refinement was carried out using a two phase model, consisting of $Ba_2SbYb(PO_4)_4$ and the $YbPO_4$ which crystallize with the $I4_1/amd$ space group. It should be noted that only high-intensity diffraction peaks of the $YbPO_4$ appear as impurity in the XRD pattern. This last refinement leads to acceptable reliability factors ($R_B = 3.8\%$). Observed, calculated, and difference XRD patterns is shown in Fig 2. The final reliability factors and atomic parameters for [Yb] are summarised in Tables 1. Selected interatomic distances and calculated bond valence sum BVS is given in Table 2.
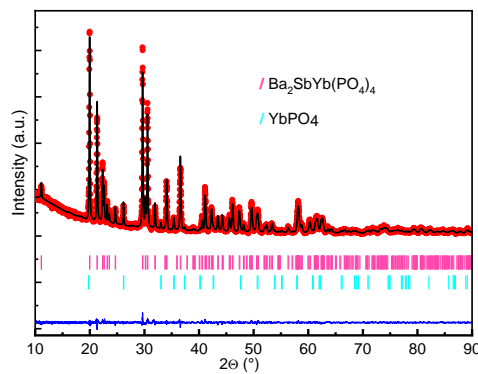
Fig.2. Rietveld refined diffraction patterns of $Ba_2SbYb(PO_4)_4$.

Table 1. Crystallographic data of $Ba_2SbM(PO_4)_4$ (M= Sc, Yb)(C2/m space group and Z=2)

Ba$_2$SbM(PO$_4$)$_4$ (M= Sc, Yb)	[Sc]	[Yb]
a(Å)	8.2924(1)	8.3451(1)
b(Å)	5.2344(3)	5.2651(3)
c(Å)	7.8787(1)	7.9772(8)
β(°)	93.8(1)	94.2(1)
V(Å^3)	340(1)	350(2)
R$_P$	0.086	0.074
R$_{WP}$	0.113	0.099
R$_B$	0.032	0.038
R$_F$	0.025	0.024

Table 2. Selected interatomic distances (Å) and calculated Bond Valence Sum (BVS) for Ba$_2$SbM(PO$_4$)$_4$.

Ba$_2$SbM(PO$_4$)$_4$ (M= Sc, Yb)	[Sc]	[Yb]
X-O = Sb(M)-O distances (Å)		
2×X-O(2)	1.911(5)	1.930(1)
4×X-O(3)	2.038(3)	2.199(4)
Aver.<X-O>	**2.00(1)**	**2.11(1)**
BVS(X)	**4.67**	**4.19**
(should be)	(4)	(4)
P-O distances (Å)		
P-O(1)	1.561(6)	1.545(6)
P-O(2)	1.528(1)	1.544(1)
2×P-O(3)	1.571(6)	1.528(4)
Aver.<P-O>	**1.55(1)**	**1.54(1)**
BVS(P)	**4.7**	**4.98**
(should be)	(5)	(5)
Ba-O distances (Å)		
2×Ba-O(1)	2.821(6)	2.691(1)
4×Ba-O(3)	2.792(4)	2.780(2)
4×Ba-O(1)	3.170(3)	3.172(3)
Aver.<Ba-O>	**2.95(1)**	**2.92(1)**
BVS (Ba)	**1.85**	**2.08**
(should be)	(2)	(2)

3.2 Structure description of Ba$_2$SbM(PO$_4$)$_4$ (M= Sc and Yb)

The structure of Ba$_2$SbM(PO$_4$)$_4$ (M= Sc and Yb) phases is represented in Fig 3. It consists of three types of polyhedra, BaO$_{10}$, PO$_4$ and Sb(M)O$_6$. The Sb(M)O$_6$ octahedra and PO$_4$ tetrahedra are interconnected via corner-sharing, alternating along the c-axis with layers of Ba cations in

ten-fold coordination (Figure 3). The ten oxygens in each BaO_{10} polyhedra are from six PO_4 phosphate groups. Eight of the oxygen atoms come from four bidentate PO_4 groups and the other two oxygen atoms belong to the other two mono-dentate PO_4 groups. P-O bond length within PO_4 tetrahedra are in good agreement with those found in other orthophosphates [17-21, 23]. The mean of Sb(M)–O distance in Sb(M)O_6 octahedra, are consistent with the crystal radii values of Sb^{5+} and M^{3+} ions in six coordination [24]. In BaO_{10} polyhedron, the Ba–O distances values can be divided to two groups (Table 3). The first group contains six relatively shortest Ba–O distances values which are around 2.80 Å for [Sc] and between 2.69 and 2.78 Å for [Yb]. The second group is formed by four longer Ba–O distances with a mean values around 3.16 Å. Therefore, the co-ordinence of Ba atoms in $Ba_2SbM(PO_4)_4$ (M= Sc,Yb) can be considered as 6 + 4.

In order to have more structural information, the bond valence sum (BVS) based on bond-strength analysis [25] for [Sc] and [Yb] were computed. The BVS values calculated for Ba, Sc, Yb, Sb, and P (Table 3) are relatively consistent with the expected formal oxidation state of Ba^{2+}, Sc^{3+}, Yb^{3+}, Sb^{5+}, and P^{5+} ions.

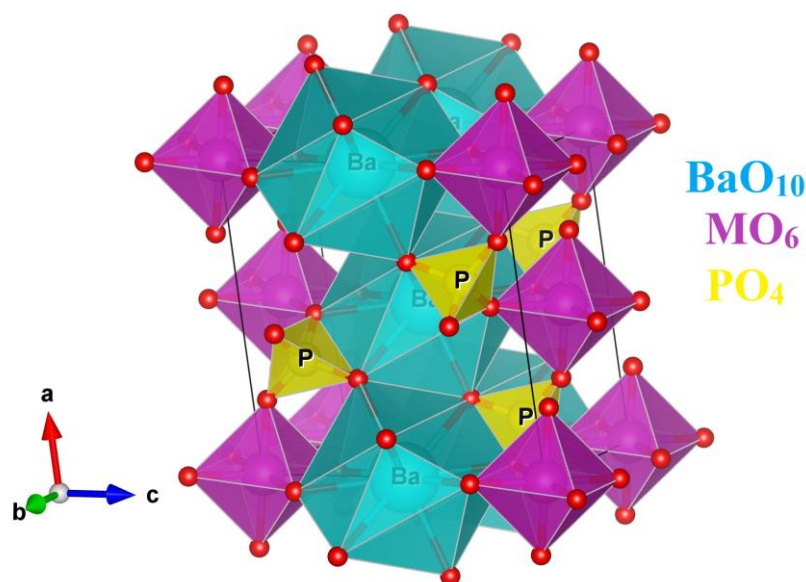**Fig.3.** Crystal structure with (M= Sb(Sc) and Sb(Yb))

4   Conclusion

In conclusion, $Ba_2SbM(PO_4)_4$ (M= Sc, Yb) phosphates are prepared by solid-state reaction method and characterised by X-ray powder diffraction. The structural characterization shows that the three phases crystallize in the yavapaiite-type structure (*C2/m* space group, (Z=2)). Its structure consists of three dimensional array of dense slabs of Sb(M)O_6 octahedra and PO_4 tetrahedra which are interconnected via corner-sharing and alternating along the c-axis with layers of Ba cations in ten-fold coordination.

6

References

1. [1] Y. Li, B. Yu, H. Wang, Y. Wang,Structural and optical characteristics of novel rare-earth-free red-emitting BaSn(PO$_4$)$_2$: Mn^{4+} phosphor, J. Molecular. Structure., 1229 (2021) 129839-129848.
2. [2] G. Blasse, G.J. Dirksen, The luminescence of barium titanium phosphate, BaTi(PO$_4$)$_2$,J. Chem. Phys. Lett., 62(1) (1979) 19-20.
3. [3] C.R. Miao, C.C. Torardi, A New High-Efficiency UV-Emitting X-Ray Phosphor, BaHf$_{1-x}$Zr$_x$(PO$_4$)$_2$,J. Solid State Chem., 155(1) (2000) 229–232.
4. [4] D. Zhao, F. X. Ma, H. Yang, W. Wei, Y. C. Fan, L. Zhang, X. Xin, Structure twinning, electronic and photoluminescence properties of yavapaiite-type orthophosphate BaTi(PO$_4$)$_2$,J. Phys. Chem. Solid. 99 (2016) 59-65.
5. [5] W.-L. Zhang, C.-S. Lin, Z. Z. He, H. Zhang, Z. Z. Luo, W.-D. Cheng, Synthesis of three members of A$^{(II)}$M$^{(IV)}$(PO$_4$)$_2$: luminescence properties of PbGe(PO$_4$)$_2$ and its Eu^{3+} doped powders,J. Cryst. En. Comm., 15 (2013) 7089–7094.
6. [6] Y. Jiang, L. Wei, C. Xiyu, S. Ge, C. Lixin, G. Rongjie, Synthesis and luminescence of β-SrGe(PO$_4$)$_2$:RE (RE=Eu^{2+}, Eu^{3+}, Tb^{3+}) phosphors for UV light-emitting diodes, J. Rare Earths, 35(2) (2017) 142–148.
7. [7] A.H. Abdeldaim, D.I. Badrtdinov, A.S. Gibbs, P. Manuel, H.C. Walker, M.D. Le, C.H. Wu, D. Wardecki, S.-G. Eriksson, Y.O. Kvashnin, Large easy-axis anisotropy in the one-dimensional magnet BaMo(PO$_4$)$_2$, J. Phys. Rev. B: Condens. Matter.100 (2019) 214427, J. Phys. Rev. B., 100 (2019) 214427.
8. [8] K. Popa, R.J. M. Konings, P. Boulet, D. Bouëxière, A.F. Popa, The high temperature behavior of barium zirconium diorthophosphate, J. Thermochim. Acta., 436(1-2) (2005) 51–55.
9. [9] K. Popa, H. Leiste, T. Wiss, R. J.M. Konings, Hydrothermal alteration of Ba$_x$M$^{IV}_x$Ce$_{2-2x}$(PO$_4$)$_2$ [M^{IV}=Zr, Hf] as hosts for minor actinides, J. Radioanal. Nucl. Chem., 273 (2007) 563–567.
10. [10] A. Leclaire, M. M. Borel, J. Chardon, B. Raveau,A Mo$^{(IV)}$ Monophosphate, BaMo(PO$_4$)$_2$, with the Yavapaiite Layer Structure,J. Solid State Chem., 116 (1995) 364-368.
11. [11] K. Popa, G. Wallez , D. Bregiroux, P. Loiseau, M^{II}Ge(PO$_4$)$_2$ (M=Ca, Sr, Ba): Crystal structure, phase transitions and thermal expansion, J. Solid State Chem., 184(10) (2011) 2629-2634.
12. [12] D. Zhao, H. Zhang, Z. Xie , W.L. Zhang, S.L. Yang, W.D. Cheng, Synthesis, crystal and electronic structures of compounds AM(PO$_4$)$_2$(A = Sr, M = Ti, Sn; A = Ba, M = Sn),J. Dalton Trans., 27 (2009) 5310-5318.
13. [13] K. Popa, R.J.M. Konings, O. Benes, T. Geisler, A.F. Popa, Thermodynamic and spectroscopic studies on the phase transition of BaHf(PO$_4$)$_2$, J. Thermochim.Acta., 451(1-2) (2006) 1–4.

14. [14] K. Fukuda, A. Moriyama, T. Iwata, Crystal structure, phase transition and anisotropic thermal expansion of barium zirconium diorthophosphate, BaZr(PO$_4$)$_2$, J. Solid State Chem., 178(6) (2005) 2144-2151.
15. [15] D. Bregiroux, K. Popa, G. Wallez, Crystal chemistry of M^{II}M^{rIV}(PO$_4$)$_2$ double monophosphates, J. Solid State Chem. 230 (2015) 26-33.
16. [16] E.J. Graeber, A. Rosenzweig, The crystal structures of yavapaiite, KFe(SO$_4$)$_2$ and goldichite, KFe(SO$_4$)$_2$·4H$_2$O, J. Am. Meniral,J. Am. Mineralog., 56 (1971) 1917–1933.
17. [17] A. Aatiq, M.R. Tigha, R. Fakhreddine, D. Bregiroux, G. Wallez, Structure, infrared and Raman spectroscopic studies of newly synthetic A^{II}(Sb$^V_{0.5}$Fe$^{III}_{0.5}$)(PO$_4$)$_2$ (A= Ba, Sr, Pb) phosphates with yavapaiite structure, J. Solid. State. Sciences, 58 (2016) 44-54.
18. [18] R. Fakhreddine, A. Aatiq., Structure, Infrared and Raman spectroscopic studies of the new Ba(Nb$^V_{0.5}$M$^{III}_{0.5}$)(PO$_4$)$_2$ (M^{III} = Al, Cr, Fe, In) yavapaiite compounds 'series, Mediterr. J. Chem.,8 (2019) 397-408.
19. [19] H. Bellefqih, R. Fakhreddine, R. Tigha, A. Aatiq.,Structure, Infrared and Raman spectroscopic studies of new A^{II}(Sb$^V_{0.5}$Cr$^{III}_{0.5}$)(PO$_4$)$_2$(A = Ba, Sr, Pb) yavapaiite phases,Mediterr. J. Chem., 10(8) (2020) 734-743.
20. [20] R. Fakhreddine, A. Ouasri, A. Aatiq, Synthesis, structural, morphology, spectroscopic and optical study of new metal orthophosphate M^{II}(Sb$_{0.5}$Ga$_{0.5}$)(PO$_4$)$_2$ (M^{II}= Sr, Pb, Ba) compounds J. Solid state chemistry, 329 (2024) 124439.
21. [21] A. Aatiq, H. Bellefqih, A. Marchoud, R. Fakhreddine, N. Boudar, R. Tigha., Structure of two new K$_2$SnX(PO$_4$)$_3$ (X = Cr, In) Langbeinite-type phases,J. Mater. Environ. Sci., 8 (2017) 2940-2945.
22. [22] J. Rodriguez-Carvajal, FULLPROF.2k: Rietveld, profile matching and integrated intensity refinement of X-ray and neutron data, V 1.9c, Laboratoire Le´on Brillouin, CEA, Saclay, France, 2001.
23. [23] A. Akhrouf, S. Krimi, M. Bouhbou, Y. Laajali, E. Hlil., Synthesis, crystal structure, optical, color, thermal, magnetic, and spectroscopic properties of the substituted honeycomb-lattice BaNi$_{2-x}$Cox(PO$_4$)$_2$ (x = 0, 0.5 and 1),J. Ceramics. International., 23 (2023) 5130-5145.
24. [24] R.D. Shannon, Revised effective ionic radii and systematic studies of interatomic distances in halides and chalcogenides, J. Acta. Cryst A. 32 (1976) 751-767.
25. [25] I.D. Brown, D. Altermatt, I.D. Brown, D. Altermatt, Bond-valence parameters obtained from a systematic analysis of the Inorganic Crystal Structure Databases, J. Acta Cryst. B41 (1985) 244 247.